JACS
JOURNAL OF THE AMERICAN CHEMICAL SOCIETY
Communication
pubs.acs.org/JACS

Epitaxial Thin Films of $ATiO_{3-x}H_x$ (A = Ba, Sr, Ca) with Metallic Conductivity

Takeshi Yajima,[†] Atsushi Kitada,[†] Yoji Kobayashi,[†] Tatsunori Sakaguchi,[†] Guillaume Bouilly,[†] Shigeru Kasahara,[‡] Takahito Terashima,[‡] Mikio Takano,[§] and Hiroshi Kageyama*[,†,§]

[†]Department of Energy and Hydrocarbon Chemistry, Graduate School of Engineering, Kyoto University, Nishikyo-ku, Kyoto 615-8510, Japan

[‡]Research Center for Low Temperature and Materials Sciences, Kyoto University, Sakyo-ku, Kyoto 606-8501, Japan

[§]Institute for Integrated Cell-Material Sciences, Kyoto University, Sakyo-ku, Kyoto 606-8501, Japan

Supporting Information

ABSTRACT: Epitaxial thin films of titanium perovskite oxyhydride $ATiO_{3-x}H_x$ (A = Ba, Sr, Ca) were prepared by CaH_2 reduction of epitaxial $ATiO_3$ thin films deposited on a $(LaAlO_3)_{0.3}(SrAl_{0.5}Ta_{0.5}O_3)_{0.7}$ substrate. Secondary ion mass spectroscopy detected a substantial amount and uniform distribution of hydride within the film. $SrTiO_3$/LSAT thin film hydridized at 530 °C for 1 day had hydride concentration of 4.0×10^{21} atoms/cm^3 (i.e., $SrTiO_{2.75}H_{0.25}$). The electric resistivity of all the $ATiO_{3-x}H_x$ films exhibited metallic (positive) temperature dependence, as opposed to negative as in $BaTiO_{3-x}H_x$ powder, revealing that $ATiO_{3-x}H_x$ are intrinsically metallic, with high conductivity of 10^2–10^4 S/cm. Treatment with D_2 gas results in hydride/deuteride exchange of the films; these films should be valuable in further studies on hydride diffusion kinetics. Combined with the materials' inherent high electronic conductivity, new mixed electron/hydride ion conductors may also be possible.

Since the discovery of ferroelectricity in $BaTiO_3$ in 1945, perovskite titanates $ATiO_3$ (A = Ba, Sr, Ca) have been the subject of extensive studies and are widely used in industry as capacitors, piezoelectric transducers, and nonvolatile memories.[1] When these insulating materials are annealed in reducing atmosphere such as flowing H_2, oxygen vacancies can be introduced,[2] giving rise to metallic behavior and even superconductivity in $SrTiO_{3-x}$.[3] Recent state-of-the-art techniques to tailor atomically controlled $SrTiO_3$ films have led to various intriguing physical properties: thermoelectricity, quantum oscillations, and field-induced superconductivity in two-dimensional electron gases.[4−6] Such films are also of technological importance for enhancing device performance.

We recently demonstrated that by CaH_2 reduction it is possible to incorporate a large amount of hydrogen into $BaTiO_3$ as an anionic solid solution, $BaTiO_{3-x}H_x$ ($x < 0.6$).[7] $SrTiO_{3-x}H_x$ and $CaTiO_{3-x}H_x$ can also be synthesized.[8] These oxyhydrides are stable in air (up to 200 °C) and water (up to 120 °C). Although the hydride ion (H^-) itself is a strong reductant, Ti in $ATiO_{3-x}H_x$ can stay at a moderate valence (+4 ∼ +3.4), commonly seen in many titanium oxides (e.g., Magnéli phases Ti_nO_{2n-1}), and is favorable for electronic conductivity. A pelletized sample of $BaTiO_{3-x}H_x$ exhibited semiconducting behavior with a room temperature (rt) resistivity $\sim 10^{-3}$–10^{-4} S/cm. The situation is in marked contrast with the cobaltate oxyhydrides, $LaSrCoO_3H_{0.7}$ and $Sr_3Co_2O_{4.33}H_{0.84}$, which have unusually low Co valences of +1.7 and are insulating due to strong repulsion of the 3d electrons.[9,10] Remarkably, the hydride ions in $ATiO_{3-x}H_x$ are exchangeable with outer gaseous hydrogen species at ∼400 °C,[7,8] implying mobile character of H^- through the perovskite network.

Unlike $LaSrCoO_3H_{0.7}$,[11] $BaTiO_{3-x}H_x$ does not have a large number of vacancies, but still seems to have good H^- diffusion within the lattice. To unveil the mechanism of H^- mobility and further explore magnetic, electric, and optical properties, experiments using single crystals or epitaxial films are crucial. Epitaxial thin-film growth also offers a possibility for applications such as mixed hydride/electronic conducting devices and hydrogen membranes.[12] However, only powder samples are available so far,[7,8] and the transport properties are not well understood in qualitative or quantitative terms. Sintered pellets cannot be used because high-temperature treatment ($T > 500$ °C) under H_2 results in decomposition. Here, we present the fabrication of epitaxial thin films of $ATiO_{3-x}H_x$ (A = Ba, Sr, Ca) by low-temperature CaH_2 reduction of the corresponding oxide films obtained using pulsed laser deposition (PLD). These films are found to be metallic down to low temperatures, with a high conductivity of $10^2 - 10^4$ S/cm at rt. Hydride exchangeability with H_2 gas is also demonstrated. We expect that many future studies on H^- diffusion kinetics can be conducted by examining these films.

Precursor oxide films of insulating $ATiO_3$ (A = Ba, Sr, Ca) were grown epitaxially on a $(LaAlO_3)_{0.3}(SrAl_{0.5}Ta_{0.5}O_3)_{0.7}$ (LSAT) substrate by PLD with $ATiO_3$ targets.[13] LSAT was employed because of the small lattice mismatch with $ATiO_3$ and for its inertness against CaH_2; i.e., the substrate remains insulating. To prepare the precursor targets, $ATiO_3$ powder (Rare Metallic 99.9%) was pressed into pellets and then sintered at 1200 °C for 48 h in air. Deposition was conducted with a KrF excimer laser pulse with $\lambda = 248$ nm. The laser energy density was 0.7 J/cm^2, and the frequency was 1 Hz. The substrate temperature during the deposition of the $ATiO_3$ thin

Received: March 13, 2012
Published: May 7, 2012

   dx.doi.org/10.1021/ja302465c | J. Am. Chem. Soc. 2012, 134, 8782–8785

film was set to 700 °C, while the O_2 partial pressure was kept at 5.0×10^{-2} Pa. The as-grown film was embedded with 0.2 g of CaH_2 in an evacuated Pyrex tube in a N_2-filled glovebox. The tube was sealed in a vacuum ($<2 \times 10^{-2}$ Pa), kept at 300−530 °C for 1 day, and then cooled to rt. Excess CaH_2 and CaO byproduct on the film surface were removed by washing with anhydrous acetone. After the hydride treatment, the colorless thin film changes to black regardless of the reduction temperature applied. Hydride reduction of thin-film oxides has been demonstrated previously, yielding $SrFeO_2$, $LaNiO_2$, and TiO_{2-x} from $SrFeO_3$, $LaNiO_3$, and TiO_2, respectively,[14,15] but H^- incorporation into oxide thin films beyond defect concentration levels has not been accomplished yet.[16]

$2\theta-\theta$ X-ray diffraction (XRD) measurements with Cu Kα radiation were performed at rt on both as-grown and hydride-treated films. XRD patterns of as-grown $SrTiO_3$/LSAT film (Figure 1a) were indexed by (00l) reflections of $SrTiO_3$, in addition to those from the substrate, indicating successful growth of epitaxial $SrTiO_3$ film. The out-of-plane lattice parameter of as-grown film was c = 3.964 Å, slightly larger than that of bulk (3.905 Å) due to in-plane compression resulting from the smaller lattice parameter of the LSAT substrate (3.868 Å), and in agreement with values previously reported.[13,17] Likewise, epitaxial thin films of $BaTiO_3$/LSAT (c = 4.083 Å) and $CaTiO_3$/LSAT (c = 3.791 Å) were fabricated. We also confirmed epitaxial growth of the films by in-plane XRD.

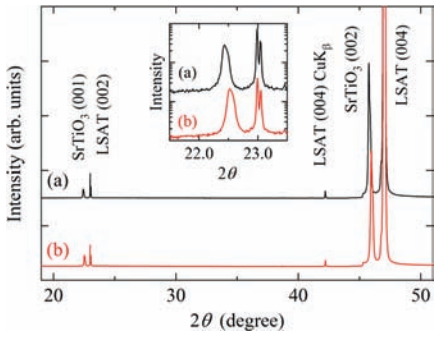

Figure 1. Out-of-plane XRD patterns of $SrTiO_3$/LSAT thin film: (a) as-grown and (b) after reduction/hydridization at 530 °C for 1 day. Inset: enlarged view with a logarithmic scale.

Figure 1b shows XRD patterns of the $SrTiO_3$/LSAT film treated with CaH_2 at 530 °C for 1 day. The full width at half-maximum of the 001 peak is ∼0.1°, almost the same as that of the as-grown film, indicating retained crystallinity during reduction. The c-axis (3.949 Å) decreases relative to the as-grown film (Δc = −0.008 Å). The degree of lattice change depends on the reduction temperature. Notably, the decrease of the c-axis in $SrTiO_3$ on LSAT occurred even when reduced at 300 °C (Figure S2). Changes in the c-axis were also seen in hydride-treated $BaTiO_3$/LSAT (Δc = −0.008 Å) and $CaTiO_3$/LSAT (Δc = +0.018 Å) (Figure S1).

The lattice change after hydride reduction might be due to an annealing effect where the parent oxide has not yet relaxed rather than due to the CaH_2 treatment. To check this, as-grown $SrTiO_3$/LSAT film was annealed at 530 °C for 1 day without CaH_2 in an evacuated Pyrex tube. In this case, Δc was less than ±0.005 Å (Table S1), implying that the change is most likely related to compositional change (i.e., O^{2-}/H^- exchange as mentioned later). Hydride-reduced $CaTiO_3$/LSAT shows lattice expansion, as expected from results of powder samples of $CaTi(O,H)_3$.[8] Hydride-treated $SrTiO_3$/LSAT and $BaTiO_3$/LSAT, in contrast, exhibit lattice contraction.[7,8] The opposite tendency of the film (vs powder) is thus remarkable and might be explained in terms of substrate-induced strain.

It is naturally expected that hydride-treated $ATiO_3$/LSAT films also incorporate a large amount of H^- at the anionic (oxygen) site. In our previous study with powder samples, neutron diffraction and quadrupole mass spectroscopy were used to quantify the H^- concentration. In the present study, we use secondary ion mass spectroscopy (SIMS) to determine the amount of H^- within the film and its depth dependence. Figure 2 shows the dynamic SIMS depth profiles of Sr, Ti, O, H ions in $SrTiO_3$/LSAT film treated at 530 °C for 1 day as a typical example. The intensity of the H secondary ion signal was converted into ion density by using a standard sample prepared by ion implantation, and the depth was estimated from the sputter rate for pristine $SrTiO_3$.

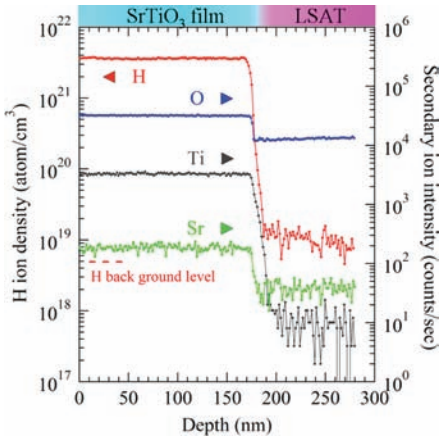

Figure 2. Dynamic SIMS depth profiles of H, Sr, Ti, O secondary ions in $SrTiO_3$/LSAT film, hydride-reduced at 530 °C for 1 day, showing uniform and substantial H^- incorporation with a composition corresponding to $SrTiO_{2.75}H_{0.25}$. The depth resolution is ∼10 nm.

The secondary ion intensity of Ti drastically decreased at ∼180 nm, corresponding to the interface between $SrTiO_3$ film and LSAT substrate. This is also supported by a drastic decrease in Sr and O signals. Constant intensity of Sr, Ti, O along the depth direction within the $SrTiO_3$ film region indicates that the phase was uniform in composition and no decomposed sections were formed upon hydride reduction.

The hydrogen density in hydride-treated $SrTiO_3$ film is 4.0×10^{21} atoms/cm^3, constant at all depths. The observed density in the film region is >2 orders of magnitude larger than in the LSAT substrate region, where the hydrogen density is background level, consistent with the fact that LSAT is not reduced by CaH_2. Previous SIMS experiments show that $BaTiO_3$ and $SrTiO_3$ films under H_2 gas atmosphere contain protons, but with much smaller quantities, $\sim 10^{20}$ atoms/cm^3 (∼0.5% H in $SrTiO_3$).[18] The hydrogen content in our $SrTiO_{3-x}H_x$ film is almost 2 orders of magnitude greater than in the protonated films, close to $\sim 10^{22}$ atoms/cm^3 ($BaTiO_{2.4}H_{0.6}$).[7] Given the synthesis environment and incorporated hydrogen amount, the hydrogen species in the hydride-treated $SrTiO_3$/LSAT film are most likely H^-, not proton or hydroxide. Hence, together with the previous results on powder,[7,8] we conclude $SrTiO_{2.75}H_{0.25}$ as the chemical composition.

dx.doi.org/10.1021/ja302465c | J. Am. Chem. Soc. 2012, 134, 8782−8785

SIMS profiles (Figure S3) for CaH_2-treated $BaTiO_3$ and $CaTiO_3$ prove also that the amount of hydrogen is several orders of magnitude greater than that of the LSAT substrate (background level, see above) and that its concentration is uniform. In SIMS measurements, chemical matrices affect sputter ion yields; thus, the overall composition must be taken into account when quantifying species. The absence of a hydrogen quantification standard for $BaTiO_3$ and $CaTiO_3$ hampered precise determination of hydrogen content. However, since all the films have the same chemical matrix except for A-site cation, we expect that the ion yields do not differ significantly. Applying the $SrTiO_3$ standard to the Ba and Ca samples results in hydrogen density of 1.0×10^{22} atoms/cm^3 for Ba ($BaTiO_{2.36}H_{0.64}$) and 1.2×10^{22} atoms/cm^3 for Ca ($CaTiO_{2.31}H_{0.69}$).

Resistivity was measured along the in-plane direction by a four-probe method. Au(30 nm)/Ti(5 nm) electrodes were deposited by electron beam deposition. Figure 3 shows

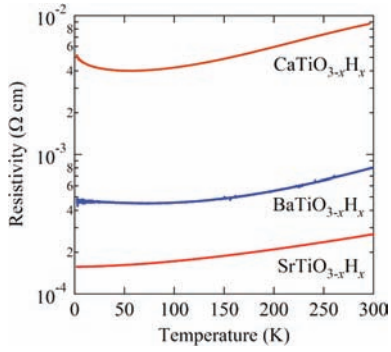

Figure 3. Typical temperature dependence of resistivity for reduced and H^--incorporated films: $SrTiO_{2.75}H_{0.25}$/LSAT, $BaTi(O,H)_3$/LSAT, and $CaTi(O,H)_3$/LSAT.

temperature dependence of the resistivity of $ATiO_{3-x}H_x$/LSAT films. All the films are highly conductive ($10^2 - 10^4$ S/cm). Notice again that the LSAT substrate is an insulator even after the hydride reduction. While semiconducting behavior was observed in a powder sample of $BaTiO_{2.4}H_{0.6}$,[7] the electrical resistivities of all of the films examined have positive temperature dependence, indicating that they are all metallic. Although we know that lattice mismatch sometimes affects transport properties,[19] $SrTiO_{3-x}H_x$/LSAT, which has the smallest lattice mismatch (vs LSAT), exhibits metallic conductivity, implying that the metallicity is intrinsic for bulk $SrTiO_{3-x}H_x$. In $SrTiO_{2.75}H_{0.25}$/LSAT film, the observed resistivity at rt and positive temperature coefficient are comparable with those of 20% Nb-doped $SrTiO_3$ films (10^3–10^4 S/cm), where the doping level should be similar.[20] $SrTiO_{3-\delta}$ is known to be a superconductor ($T_c \approx 0.5$ K),[3] but due to instrumental limits, we currently cannot verify whether our oxyhydride films are also superconducting. Bulk $BaTiO_{3-x}H_x$ and $CaTiO_{3-x}H_x$ are also expected to show metallic temperature dependence. The semiconducting behavior previously observed in powder samples of $BaTiO_{3-x}H_x$ would involve a large influence from grain boundaries, as they consist of a collection of small 170 nm particles.

Generally, in oxides, the randomness induced by oxygen vacancies affects the electronic conductivity more than cation substitution. For instance, Nb doping in TiO_2 and $SrTiO_3$ results in 90% carrier activation;[21,22] however, oxygen deficiency in $SrTiO_3$ results in <60% carrier activation.[23] Hall measurements for $SrTiO_{2.75}H_{0.25}$ indicate a carrier density of 4.1×10^{21} cm^{-3} at 300 K (Figure S4). This corresponds reasonably well with the H^- amount observed with SIMS. Based on powder studies,[7] there should be few oxygen vacancies, so the carriers should primarily be due to H^- rather than vacancy doping. As in Nb-doped (i.e., cation-doped) $SrTiO_3$, carrier activation in our oxyhydride sample is also very high. While large amounts of oxygen vacancies readily induce a random potential that is detrimental to electronic conductivity, H^- with the close ionic radius to O^{2-}, results in significantly less random potential, even at high doping levels. Another advantage of H^- as a dopant is the ability to generate high carrier concentrations. High carrier amounts from oxygen vacancies are not possible for structural reasons. For example, oxygen vacancies >1.5 at.% result in collapse of the perovskite framework.[24] However, using H^- as dopant keeps the anion sites full, removing such limits on doping.

Transport properties of H^--incorporated films exhibit prominent A-cation dependence, with rt resistivity descending as Ca > Ba > Sr (Figure 3). The H^- amount and degree of lattice mismatch with LSAT substrate could account for this behavior. Furthermore, for $CaTiO_{3-x}H_x$/LSAT film, a change in sign of the $\rho-T$ slope was observed at ~50 K. Such crossover behavior has been reported in thin films of La-doped $SrTiO_3$ and other titanium oxides, for which various origins such as tunneling effects in the percolation model have been discussed.[25,26] The origin of the crossover behavior in the $\rho-T$ curve of $CaTiO_{3-x}H_x$/LSAT should be clarified in future work.

There is a notable difference in electrical conductivity between $BaTiO_{3-x}H_x$ and $BaTiO_{3-x}$. For $BaTiO_{3-x}$, metallic behavior was first reported by Kolodiazhnyi, perhaps with very few oxygen vacancies.[27] However, this metallic state is accompanied by several ferroelectric transitions (leading to symmetry changes), resulting in distinct anomalies in the $\rho-T$ curves. In contrast, $BaTiO_{3-x}H_x$/LSAT film exhibits a smooth temperature dependence of resistivity, indicating the absence of any structural change down to 2 K. Filling a large amount of vacancies with an anion (i.e., H^-) seems to suppress these transitions. We also note the conductivity of $BaTiO_{3-x}H_x$/LSAT ($10^3 - 10^4$ S/cm) is 2–5 orders of magnitude more than that of $BaTiO_{3-x}$.

To investigate H^- exchangeability, $SrTiO_{2.89}H_{0.11}$/LSAT film was annealed with deuterium gas at 420 °C for 6 h in an evacuated Pyrex tube. To eliminate residual O_2 and H_2O in our previous flowing D_2 setups, a small physically separated amount of CaD_2 was sealed in a tube with the $SrTiO_{2.89}H_{0.11}$/LSAT film. Upon heating, CaD_2 decomposed and served as a D_2 gas source. Figure 4 shows dynamic SIMS depth profile measurements of the film after D_2 treatment. An almost uniform distribution of deuteride ions along the depth direction is observed in the film region. The hydride and deuteride ion densities in the film region are 3.0×10^{20} and 1.5×10^{21} atoms/cm^3, respectively. Exchange of O^{2-} for H^-/D^- with H_2 (D_2) gas is highly unlikely at this temperature, as demonstrated in powder sample.[7] The H/D exchange ratio, D/(H+D), was 83%, which is almost the same as in bulk $BaTiO_3$ (90%). The total hydride ion density (H+D) is almost the same as the original $SrTiO_{2.89}H_{0.11}$/LSAT film, indicating deuteride exchange without any change in composition such as oxidation. The success of such hydride exchange in the oxyhydride film provides us an opportunity to clarify their diffusion kinetics by examining films with H/D concentration gradients.

dx.doi.org/10.1021/ja302465c | J. Am. Chem. Soc. 2012, 134, 8782–8785

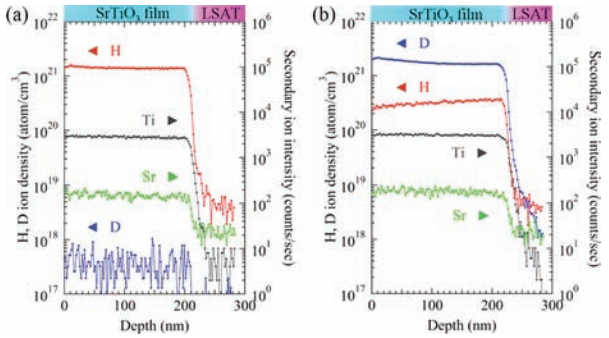

Figure 4. Dynamic SIMS depth profile of H, D, Sr, Ti secondary ions in (a) $SrTiO_{2.89}H_{0.11}$/LSAT and (b) $SrTiO_{2.89}H_{0.02}D_{0.09}$/LSAT, obtained by deuterization of $SrTiO_{3-x}H_x$/LSAT at 420 °C for 6 h.

In conclusion, SIMS experiments indicate a large amount of hydride (e.g., 4.0×10^{21} atoms/cm^3 for A = Sr), uniform distribution in the films, and the ability of hydride to exchange with H_2 gas. Metallic conductivity (10^2–10^4 S/cm) was observed in a wide temperature range down to 2 K. Incorporation of hydride as a dopant allows controlling carrier levels in oxides to unprecendented amounts. This, combined with the hydride diffusion and exchange at low temperature, promises applications involving mixed electron/hydride conduction at temperatures lower than those encountered in oxide ion conduction, because the lighter mass and lower charge of hydride over oxide should make it more mobile.

With oxide ion conductors, oxide incorporation by surface reactions and their diffusion within the bulk phase and across grain boundaries have been revealed in great detail by applying a variety of experimental techniques on single crystals together with theoretical tools.[28,29] Successful growth of oxyhydride epitaxial thin films will also enable in-depth studies on hydride diffusion kinetics and equilibrium in oxides. Additionally, intriguing properties specific to thin films have been reported, including confinement effects on $SrTiO_3$ and selective oxygen migration pathways for $CaFeO_{2.5}$ with different orientations[30] and artificial superlattices.[31] Similar experiments on the oxyhydride analogue would be highly interesting.

■ ASSOCIATED CONTENT

Supporting Information

XRD patterns and typical SIMS depth profiles; and Hall coefficient data. This material is available free of charge via the Internet at http://pubs.acs.org.

■ AUTHOR INFORMATION

Corresponding Author

kage@scl.kyoto-u.ac.jp

Notes

The authors declare no competing financial interest.

■ ACKNOWLEDGMENTS

We thank the Foundation for Promotion of Material Science and Technology of Japan for SIMS measurements. This work was supported by the Japan Society for the Promotion of Science through its "Funding Program for World-Leading Innovative R&D on Science and Technology Program", from the Ministry of Education, Culture, Sports, Science and Technology of Japan. A.K. was supported by the Japan Society for the Promotion of Science for Young Scientists.

■ REFERENCES

(1) Haertling, G. H. *J. Am. Ceram. Soc.* **1999**, *82*, 797.
(2) Wild, R. L.; Rockar, E. M.; Smith, J. C. *Phys. Rev. B* **1973**, *8*, 3828.
(3) Schooley, J. F.; Hosler, W. R.; Ambler, E.; Becker, J. H.; Cohen, M. L.; Koonce, C. S. *Phys. Rev. Lett.* **1965**, *14*, 305.
(4) Kozuka, Y.; Kim, M.; Bell, C.; Kim, B. G.; Hikita, Y.; Hwang, H. Y. *Nature* **2009**, *462*, 487.
(5) Ueno, K.; Nakamura, S.; Shimotani, H.; Ohtomo, A.; Kimura, N.; Nojima, T.; Aoki, H.; Iwasa, Y.; Kawasaki, M. *Nat. Mater.* **2008**, *7*, 855.
(6) Ohta, H.; Kim, S.-W.; Mune, Y.; Mizoguchi, T.; Nomura, K.; Ohta, S.; Nomura, T.; Nakanishi, Y.; Ikuhara, Y.; Hirano, M.; Hosono, H.; Koumoto, K. *Nat. Mater.* **2007**, *6*, 129.
(7) Kobayashi, Y.; Hernandez, O. J.; Sakaguchi, T.; Yajima, T.; Roisnel, T.; Tsujimoto, Y.; Morita, M.; Noda, Y.; Mogami, Y.; Kitada, A.; Ohkura, M.; Hosokawa, S.; Li, Z.; Hayashi, K.; Kusano, Y.; Kim, J.; Tsuji, N.; Fujiwara, A.; Matsushita, Y.; Yoshimura, K.; Takegoshi, K.; Inoue, M.; Takano, M.; Kageyama, H. *Nat. Mater.* **2011**, DOI: 10.1038/NMAT3302.
(8) Sakaguchi, T.;et al., submitted.
(9) Helps, R. M.; Rees, N. H.; Hayward, M. A. *Inorg. Chem.* **2010**, *49*, 11062.
(10) Bridges, C. A.; Darling, G. R.; Hayward, M. A.; Rosseinsky, M. J. *J. Am. Chem. Soc.* **2005**, *127*, 5996.
(11) Bridges, C. A.; Fernandez-Alonso, F.; Goff, J. P.; Rosseinsky, M. J. *Adv. Mater.* **2006**, *18*, 3304.
(12) Kosacki, I.; Rouleau, C. M.; Becher, P. F.; Bentley, J.; Lowndes, D. H. *Solid State Ionics* **2005**, *176*, 1319.
(13) Nuzhnyy, D.; Petzelt, J.; Kamba, S.; Yamada, T.; Tyunina, M.; Tagantsev, A. K.; Levoska, J.; Setter, N. *J. Electroceram.* **2009**, *22*, 297.
(14) Inoue, S.; Kawai, M.; Shimakawa, Y.; Mizumaki, M.; Kawamura, N.; Watanabe, T.; Tsujimoto, Y.; Kageyama, H.; Yoshimura, K. *Appl. Phys. Lett.* **2008**, *92*, 161911.
(15) Kitada, A.; Kasahara, S.; Terashima, T.; Yoshimura, K.; Kobayashi, Y.; Kageyama, H. *Appl. Phys. Express* **2011**, *4*, 035801.
(16) Kodu, M.; Aints, M.; Avarmaa, T.; Denks, V.; Feldbach, E.; Jaaniso, R.; Kirm, M.; Maaroos, A.; Raud, J. *Appl. Surf. Sci.* **2011**, *257*, 5328.
(17) Tarsa, E. J.; Hachfeld, E. A.; Quinlan, F. T.; Speck, J. S.; Eddy, M. *Appl. Phys. Lett.* **1996**, *68*, 490.
(18) Baniecki, J. D.; Laibowitz, R. B.; Shaw, T. M.; Parks, C.; Lian, J.; Xu, H.; Ma, Q. Y. *J. Appl. Phys.* **2001**, *89*, 2873.
(19) Choi, K. J.; Biegalski, M.; Li, Y. L.; Sharan, A.; Schubert, J.; Uecker, R.; Reiche, P.; Chen, Y. B.; Pan, X. Q.; Gopalan, V.; Chen, L. Q.; Schlom, D. G.; Eom, C. B. *Science* **2004**, *306*, 1005.
(20) Ohta, H.; Sugiura, K.; Koumoto, K. *Inorg. Chem.* **2008**, *47*, 8429.
(21) Furubayashi, Y.; Hitosugi, T.; Yamamoto, Y.; Inaba, K.; Kinoda, G.; Hirose, Y.; Shimada, T.; Hasegawa, T. *Appl. Phys. Lett.* **2005**, *86*, 252101.
(22) Mune, Y.; Ohta, H.; Koumoto, K.; Mizoguchi, T.; Ikuhara, Y. *Appl. Phys. Lett.* **2007**, *91*, 192105.
(23) Gong, W.; Yun, H.; Ning, Y. B.; Greedan, J. E.; Datars, W. R.; Stager, C. V. *J. Solid State Chem.* **1991**, *90*, 320.
(24) Sinclair, D. C.; Skakle, J. M. S.; Morrison, F. D.; Smith, R. I.; Beales, T. P. *J. Mater. Chem.* **1999**, *9*, 1327.
(25) Liang, S.; Wang, D. J.; Sun, J. R.; Shen, B. G. *Solid State Commun.* **2008**, *148*, 386.
(26) Gariglio, S.; Seo, J. W.; Triscone, J. M. *Phys. Rev. B* **2001**, *63*, 161103.
(27) Kolodiazhnyi, T. *Phys. Rev. B* **2008**, *78*, 045107.
(28) Merkle, R.; Maier, J. *Angew. Chem. Int. Ed.* **2008**, *47*, 3874.
(29) Kotomin, E. A.; Alexandrov, V.; Gryaznov, D.; Evarestov, R. A.; Maier, J. *Phys. Chem. Chem. Phys.* **2011**, *13*, 923.
(30) Inoue, S.; Kawai, M.; Ichikawa, N.; Kageyama, H.; Paulus, W.; Shimakawa, Y. *Nat. Chem.* **2010**, *2*, 213.
(31) Matsumoto, K.; Haruta, M.; Kawai, M.; Sakaiguchi, A.; Ichikawa, N.; Kurata, H.; Shimakawa, Y. *Sci. Rep.* **2011**, *1*, 27.